

# Mild synthesis of mesoporous silica supported ruthenium nanoparticles as heterogeneous catalysts in oxidative Wittig coupling reactions†

Cite this: *Catal. Sci. Technol.*, 2014, 4, 435

Adela I. Carrillo,<sup>a</sup> Luciana C. Schmidt,<sup>a</sup> M. Luisa Marin<sup>ab</sup> and Juan C. Scaiano<sup>\*a</sup>

A new efficient approach for the *in situ* synthesis of anchored ruthenium nanoparticles (RuNP) in three different kinds of mesoporous silica materials, MCM-41, SBA-15 and HMS, has been developed. Solids have been synthesized under very mild conditions from RuCl<sub>3</sub>·H<sub>2</sub>O salt reduced in one hour at room temperature in the mesoporous silicas previously grafted with aminopropyltriethoxysilane (APTES). Well-dispersed ruthenium nanoparticles, with an average size of 3 nm, anchored into the silica network by the APTES were obtained. These materials, with a molar ratio of Si/Ru = 40, were found to be catalytically active and selective in the alcohol oxidation–Wittig olefination. Interestingly, while the reaction occurs from the alcohol, control experiments suggest that the aldehyde (the common Wittig substrate) is not involved.

Received 4th October 2013,  
Accepted 4th November 2013

DOI: 10.1039/c3cy00773a

www.rsc.org/catalysis

## Introduction

The development of sustainable routes for the large scale production of fine chemicals, *i.e.*, cost-effective and environmentally friendly, is one of the major current concerns at the industrial level.<sup>1</sup> The use of supported metal nanoparticles allows the combination of increased efficiency from nanoparticle catalysts, with the advantages of heterogeneous supports, leading to a ‘green catalytic process’, with higher selectivity and conversion and easy catalyst recovery.<sup>2</sup>

The design of the catalyst is the key step in the development of a sustainable catalytic reaction. Among the most crucial issues in the preparation of a nanocatalyst is avoiding agglomeration of the nanoparticles as well as leaching from the active sites of the support; this can be achieved by anchoring the nanoparticles to the support surface.

Mesoporous silicas such as MCM-41 are attractive catalyst supports because they present high surface areas where the active sites can be highly dispersed. Different strategies have been successfully employed to introduce catalytic active sites into mesoporous silicas including ion exchange, chemical vapor deposition or impregnation.<sup>3,4</sup> However, the interaction between the active site and the support is frequently very weak. This may cause leaching of the active sites into the

reaction media, potentially leading to a decrease in the catalytic activity of the material. To overcome this issue, more recently co-condensation or chemical grafting methods to covalently bond the active species into mesoporous materials are being reported. For example, the co-condensation method has been used to incorporate palladium nanoparticles into a silica matrix by functionalizing the nanoparticles with alkoxysilanes and then co-polymerizing them with tetraethoxysilanes in the presence of cationic surfactants *via* base-catalyzed hydrolysis.<sup>5</sup> Recently, the synthesis of a hybrid mesoporous material with a molybdenum complex covalently attached was reported<sup>6</sup> by using either post synthesis grafting or co-condensation approaches.

Supported ruthenium catalysts, mostly obtained by impregnation, have emerged as a new family of versatile catalysts for different chemical reactions. In fact, they have been employed in industrial processes for the synthesis of paraffins,<sup>7</sup> methanation of CO<sup>8</sup> or in the hydrogenation of benzene to cyclohexane.<sup>9</sup> Supported ruthenium nanoparticles (SRuNP) have been found to have very good catalytic activity towards the synthesis of ammonia<sup>10</sup> or hydrogenation of monoaromatics.<sup>11</sup>

In the present work, we take advantage of the activity of RuNP and mesoporous silica to prepare three new hybrid materials and explore their catalytic properties. The one-pot alcohol oxidation–Wittig reaction producing  $\alpha,\beta$ -unsaturated esters was chosen to test the catalytic activity of the materials as it is the most commonly used method for the synthesis of alkenes<sup>12</sup> and a process where catalytic routes would be important.<sup>13</sup> The new materials showed good catalytic activity in the Wittig olefination of benzyl alcohols.<sup>14</sup> The most interesting point was that reaction occurs without the intermediacy

<sup>a</sup> Department of Chemistry and Centre for Catalysis Research and Innovation, University of Ottawa, 10 Marie Curie, Ottawa, K1N 6N5, Canada.

E-mail: scaiano@photo.chem.uottawa.ca

<sup>b</sup> Instituto Universitario Mixto de Tecnología Química (UPV-CSIC), Universitat Politècnica de València. Avenida de los Naranjos s/n, 46022 Valencia, Spain

† Electronic supplementary information (ESI) available. See DOI: 10.1039/c3cy00773a

of free aldehyde and with a high selectivity for the *E* product. These new solids have been prepared by initially grafting APTES onto the surface of MCM-41, SBA-15 or HMS type silicas. Then aqueous RuCl<sub>3</sub> was stirred in the presence of the solids leading to covalently bonded RuNP that were fully characterized by BET surface area, pore size distribution, X-ray diffraction (XRD), transmission electron microscopy (TEM), X-ray photoelectron spectroscopy (XPS) and inductively coupled plasma mass spectrometry (ICP).

## Experimental

Most of the experimental details are supplied as ESI,<sup>†</sup> with only a few key details included here.

### Preparation of SRuNP

First, 1.5 g of mesoporous silica solid, MCM-41,<sup>6</sup> SBA-15<sup>15</sup> or HMS<sup>16</sup> (prepared according to already published methods, see more details in the ESI<sup>†</sup>) was dehydrated in an oven at 473 K for 2 h. Then, 50 mL of anhydrous toluene was added to the activated materials and this mixture was stirred for 1 h in order to obtain a homogeneous dispersion followed by the addition of 0.5 mL APTES and refluxed overnight. Finally, the white solid (silica-APTES) obtained was filtered, washed with fresh toluene and acetone and air-dried.

Second, ruthenium chloride (RuCl<sub>3</sub>·*x*H<sub>2</sub>O, 9 mg) was added to an aqueous mixture (110 mL) of the corresponding silica-APTES material (1.5 g). After stirring for 1 h at room temperature, the grey solids obtained were filtered and washed several times with water to remove the unreacted salt. The air-dried new SRuNP (2.3–2.5 wt% Ru, ICP determined) were denoted as Ru@MCM, Ru@SBA and Ru@HMS.

### Catalysis tests

The catalysis tests were performed using the new mesoporous silica materials. Typically, a mixture of benzyl alcohol (0.1 mL, 1.0 mmol), methyl (triphenylphosphoranylidene)acetate (334 mg, 1.0 mmol) and 50 mg of SRuNP (1.2 mol% Ru) in 2 mL of toluene was stirred for 24 h at 80 °C under an oxygen atmosphere. The yields were determined by GC-MS after filtration and addition of 1,1'-binaphthyl as an internal standard.

## Results

### Catalyst characterization

Fig. 1 compares the X-ray diffraction patterns of MCM-41, SBA-15 and HMS before and after their functionalization with anchored RuNP. In the patterns of MCM-41 type materials (Fig. 1, top), a dominant (100) peak with small (110) and (200) reflections is normally attributed to the 2D-hexagonal structure (*p6mm*).<sup>17</sup> Aminosilane grafting into MCM-41 and further incorporation of RuNP caused a considerable decrease in the XRD intensity.

TEM images of the SRuNP are shown in Fig. 2. Ru@MCM and Ru@SBA reveal the hexagonal mesoporous arrangement typical for these materials, even after incorporation of RuNP, while in the case of Ru@HMS a disordered and wormhole

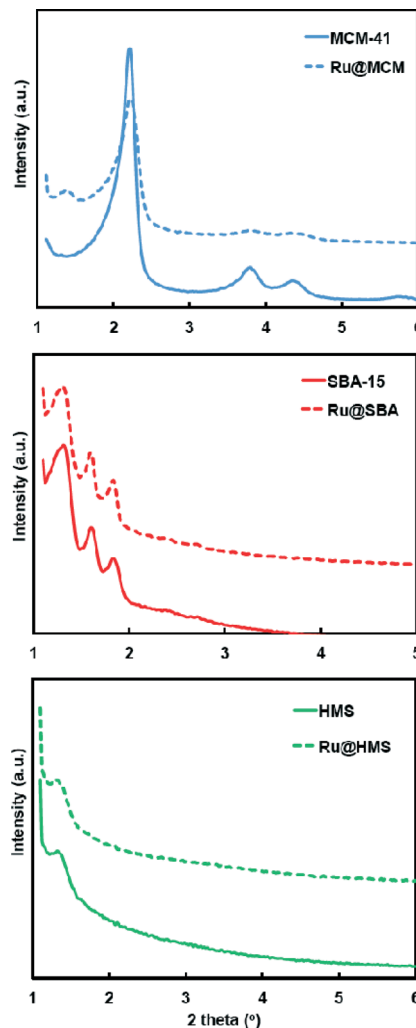


Fig. 1 Low angle XRD patterns of pure silicas: MCM-41 (top), SBA-15 (middle) and HMS (bottom) and their corresponding SRuNP materials.

mesostructure was shown.<sup>16</sup> Fig. 2 also reveals that RuNP are confined and highly dispersed into the channels of the mesoporous silica and confirms that these materials maintain the 2D-hexagonal mesopore arrangement of the pure MCM-41. The SBA-15 family of materials showed three well-defined peaks at  $2\theta$  values between 1 and 8° (Fig. 1, middle) that can be indexed as (100), (110) and (200) Bragg reflections, typical of hexagonal (*p6mm*) SBA-15.<sup>18</sup> In these materials, both the intensity and resolution of the peaks are not decreased by anchoring RuNP, probably because the size of the RuNP (*ca.* 3 nm) does not affect the pores of SBA-15

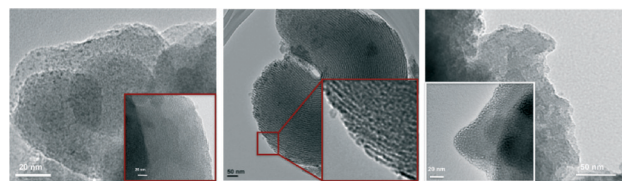


Fig. 2 TEM images of the hybrid materials Ru@MCM (left), Ru@SBA (center) and Ru@HMS (right).

(ca. 9 nm). HMS and Ru@HMS patterns show a single low-angle diffraction peak characteristic of a wormhole framework.<sup>19</sup>

The new hybrid materials exhibited type IV isotherms with a distinctive nitrogen uptake due to the capillary condensation of nitrogen inside the mesopores (Fig. 3).<sup>3</sup> Further, each material showed its characteristic features; for instance, MCM-41 solids showed a sharp increase in the adsorbed volume at  $P/P_0 = 0.2$ – $0.4$  because of the 2–3 nm diameter pores.<sup>20</sup> Otherwise, SBA-15 type materials showed an abrupt step at higher relative pressures ( $P/P_0 = 0.6$ – $0.8$ ) as expected for bigger pore size silicas.<sup>18</sup> Finally, HMS solids did not show an abrupt step in their isotherm profiles due to the broad pore size distributions.<sup>3</sup> Table 1 summarizes BJH pore size distributions calculated from the adsorption branches of the isotherms and BET surface areas of the new solids. As expected, in all cases both the pore diameter and the surface area decreased after the incorporation of the anchored RuNP into the mesopores.

Additional efforts were made to characterize the oxidation state of the SRuNP. Since the XRD experiments were inconclusive, XPS was performed on the all new materials, including the MCM-APTES that was used as the standard. According to the XPS spectra (Fig. 4) (Ru 3d<sub>5/2</sub> at 280.4 eV, and Ru 3p<sub>3/2</sub> at 462.0 eV, respectively), the ruthenium particles were at least partially in a zero oxidation state in accordance with the literature, although other states are also likely to be found.<sup>21</sup>

### Catalytic activity: alcohol oxidation–Wittig olefination

Embedded ruthenium nanoparticles in aluminum oxyhydroxide have been reported as catalysts for the one-pot alcohol oxidation–Wittig reaction producing  $\alpha,\beta$ -unsaturated esters.<sup>14</sup> In this report, the overall reaction is mediated by the aldehyde. This reaction was selected as a test to evaluate the activity of the new catalysts.

Interestingly, we were unable to oxidize benzyl alcohol to benzaldehyde using SRuNP in toluene at 80 °C under an oxygen atmosphere (with or without added Ph<sub>3</sub>PO); however, in the presence of methyl (triphenylphosphoranylidene)acetate, the reaction proceeded with the formation of the  $\alpha,\beta$ -unsaturated

ester methyl cinnamate (Scheme 1). This suggests that, in contrast with the literature example, our catalysts can yield Wittig products without free aldehyde mediation.

The reaction does not occur without using SRuNP (Table 2, entry 1) or when only the support is used as the catalyst (Table 2, entry 2). In a control experiment, the reaction was performed using aldehyde, instead of alcohol. This reaction was essentially complete after 3 h at 80 °C (1 mmol benzaldehyde, 1 mmol ylide and 1.2% mol Ru@MCM under O<sub>2</sub>); not surprisingly the catalyst is not required when the reagent is the aldehyde.

The effects of organic solvent, temperature, time of reaction, atmosphere, and Ru% on yield and stereoselectivity were investigated using Ru@MCM, as shown in Table 2.

Higher conversions were obtained when non-polar solvents such as toluene and CCl<sub>4</sub> were used. Very low yield was obtained when DMF was used (Table 2, entry 5). While using THF, no conversion was achieved even under reflux for 18 h (Table 2, entry 6). Increasing the temperature from 80 to 110 °C did not result in an increase in the conversion (Table 2, entries 4 and 7). When the reaction was performed under air, the byproduct benzyl cinnamate was obtained together with a similar yield of the desired methyl cinnamate (Table 2, entry 9), whereas, under N<sub>2</sub>, very little reaction was observed even after increasing the temperature (Table 2, entry 8). When the percentage of Ru was increased up to 1.2% the conversion enhanced up to 70% after 24 h; nevertheless, quantitative conversion could be obtained after 48 h (Table 2, entries 10 and 11).

From the data in Table 2, the reaction leads always to the *E*-methyl cinnamate as the preferred isomer. Further, in order to evaluate the scope of this reaction, different primary alcohols were used as shown in Table 3.

Finally, the nature of the silica support as well as the recyclability in the reaction of the benzyl alcohol with methyl (triphenylphosphoranylidene)acetate was tested (Table 4). MCM-41 and SBA-15 type silica showed the same conversion. Nevertheless, Ru@MCM material was more selective toward the *E*-methyl cinnamate isomer. This may reflect the smaller pore size of the MCM type silica, *i.e.*, 3 nm, against the 9 nm pore size of the SBA-15 type silica. Moreover, HMS solids showed lower conversions due to their porosity disorder. With regard to the recyclability, all the catalysts conserved 50%–60% of their original activity upon second use (Table 4).

Although the mechanism of the alcohol oxidation–Wittig olefination has not been investigated in detail in the absence of the methyl (triphenylphosphoranylidene)acetate, the benzaldehyde was not detected when the reaction of the catalyst and alcohol was attempted. On the other hand, as expected, the reaction between the aldehyde and the methyl (triphenylphosphoranylidene)acetate proceeded without the presence of the catalyst (*vide supra*).

## Discussion

Metal nanoparticles are usually prepared by reduction of the aqueous salt in the presence of a protective agent to prevent

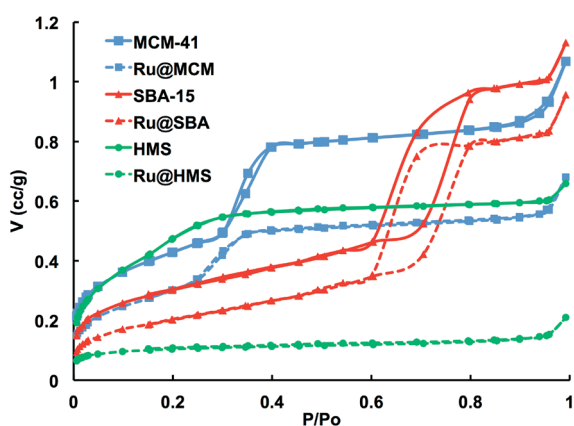
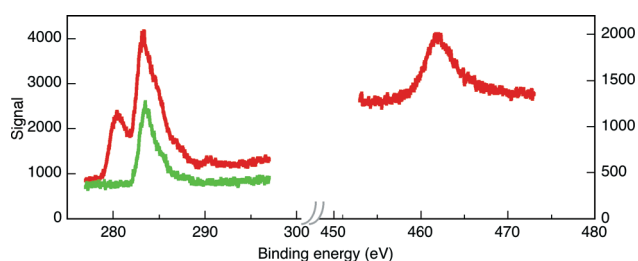


Fig. 3 Nitrogen adsorption–desorption isotherms of the synthesized materials: MCM-41, Ru@MCM, SBA-15, Ru@SBA, HMS, and Ru@HMS.

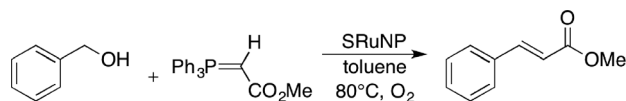
**Table 1** Textural properties and ruthenium loading of the new catalysts

Sample	$d_p^{BJH,a}$ (nm)	$A_{BET}^b$ ( $m^2 g^{-1}$ )	$V_p^{BJH,c}$ ( $cc g^{-1}$ )	Metal loading wt% <sup>d</sup>
MCM-41	3.0	995	1.1	—
Ru@MCM	2.4	740	0.7	2.3
SBA-15	9.0	785	1.2	—
Ru@SBA	8.7	430	0.8	2.5
HMS	2.0	700	0.7	—
Ru@HMS	2.0–4.0	190	0.4	2.3

<sup>a</sup> Average mesopore diameters were estimated from the adsorption branch of the nitrogen isotherm using the BJH method. <sup>b</sup> The BET surface area was estimated by multipoint BET method using the adsorption data in the relative pressure ( $P/P_0$ ) range of 0.05–0.30. <sup>c</sup> Mesopore volume from the isotherms at the relative pressure of 0.8. <sup>d</sup> Ruthenium amount determined by ICP analysis.



**Fig. 4** XPS spectra showing the C1s, Ru 3d<sub>5/2</sub> and Ru3p<sub>3/2</sub> regions of Ru@MCM (red) and MCM-APTES (green).



**Scheme 1** Alcohol oxidation-Wittig olefination.

aggregation. Literature reports indicate that RuNP could be obtained using polyols as reductants and PVP as stabilizer under microwave heating<sup>22</sup> or simply refluxing.<sup>23</sup> On the other hand, amines have been reported as useful reducing agents in the formation of AuNPs from HAuCl<sub>4</sub>, acting also as protecting agents.<sup>24</sup> Here, we have demonstrated that the two concepts can be applied to the synthesis of new hybrid heterogeneous materials based on RuNP. In fact, APTES anchored to the surface of MCM-41, SBA-15 or HMS silicas acted as both a reducing and protecting agent. The developed

**Table 3** Reaction of different primary alcohols with methyl (triphenylphosphoranylidene)acetate<sup>a</sup>

#	Alcohol	Product	Product yield % <sup>b</sup>	E/Z ratio <sup>b</sup>
1			99	32:1
2			75	18:1
3			57	6:1
4			45	10:1
5			40	2:1
6			65	—

<sup>a</sup> Primary alcohol (0.1 mL, 1.0 mmol), methyl (triphenylphosphoranylidene)acetate (334 mg, 1.0 mmol) and 1.2 mol% of Ru@MCM in 2 mL of toluene, under an oxygen atmosphere for 24 h. <sup>b</sup> The product yields were determined by gas chromatography using 1,1'-binaphthyl as internal standard, error <5%.

**Table 2** Reaction of benzyl alcohol with methyl (triphenylphosphoranylidene)acetate<sup>a</sup>

#	Catalyst (mol%)	Solvent	Conditions time	Conv. <sup>b</sup> (%)	Product yield <sup>c</sup> (%)	E/Z ratio <sup>d</sup>
1	None	Toluene	80 °C, O <sub>2</sub> /18 h	0	—	—
2	MCM-APTES	Toluene	80 °C, O <sub>2</sub> /18 h	0	—	—
3	0.4	CCl <sub>4</sub>	80 °C, O <sub>2</sub> /18 h	32	27	Not quantified
4	0.4	Toluene	80 °C, O <sub>2</sub> /18 h	49	49	11:1
5	0.4	DMF	80 °C, O <sub>2</sub> /18 h	12	12	11:1
6	0.4	THF	Reflux/18 h	0	—	—
7	0.4	Toluene	110 °C, O <sub>2</sub> /18 h	34	31	10:1
8	0.4	Toluene	110 °C, N <sub>2</sub> /18 h	10	Not quantified	Not quantified
9	0.4	Toluene	80 °C, air/18 h	48	40 <sup>d</sup>	11:1
10	1.2	Toluene	80 °C, O <sub>2</sub> /24 h	70	61	17:1
11	1.2	Toluene	80 °C, O <sub>2</sub> /48 h	100	81	16:1

<sup>a</sup> Benzyl alcohol (0.1 mL, 1.0 mmol), methyl (triphenylphosphoranylidene)acetate (334 mg, 1.0 mmol) and the state amount of Ru@MCM in 2 mL of solvent. <sup>b</sup> Quantification of unreacted benzyl alcohol. <sup>c</sup> The product methyl cinnamate was determined by GC using 1,1'-binaphthyl as the internal standard, error <5%. <sup>d</sup> Together with benzyl cinnamate product of transesterification.

**Table 4** Recyclability of SRuNP in the reaction of the benzyl alcohol with methyl (triphenylphosphoranylidene)acetate

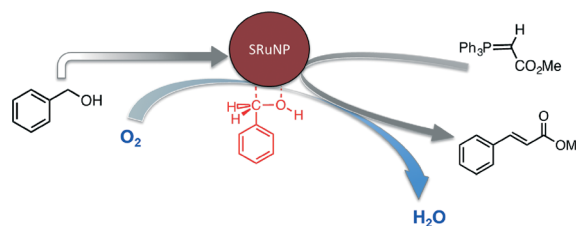
Catalyst	Conversion (%)	<i>E/Z</i> ratio	% reuse
Ru@MCM	70.0	17 : 1	50
Ru@SBA	70.0	11 : 1	60
Ru@HMS	55.0	17 : 1	60

protocol is simple and mild since stirring for just 1 hour at room temperature was enough to reduce the Ru(III) salt and incorporate the resulting RuNP into the mesoporous silica solids. The properties of the materials obtained, Ru@MCM, Ru@SBA and Ru@HMS include defined particle size and narrow distribution.<sup>25</sup> TEM images (Fig. 2) showed that RuNP are embedded into the pores of the solids, thus inhibiting the agglomeration of the nanoparticles and the subsequent loss of activity. Incorporating the RuNP into the silica mesopores led to the expected decrease of the surface of the final solid. Nevertheless, 740 m<sup>2</sup> g<sup>-1</sup> for Ru@MCM was much higher than the 424.7 m<sup>2</sup> g<sup>-1</sup> reported for the analogous heterogeneous Ru(0) catalyst Ru/AlO(OH).<sup>26</sup> XPS measurements performed on the all new materials, including the MCM-APTOS were consistent with the presence of Ru(0). As shown in Fig. 4, the bands at 280.4 eV and 462.0 eV can be attributed to the Ru 3d<sub>5/2</sub> and Ru 3p<sub>3/2</sub>, respectively.<sup>21,23</sup>

Although the Wittig reaction is used worldwide as the most common method to prepare alkenes, the mechanism involved is still under scrutiny.<sup>12,27</sup> In particular, ruthenium complexes have already been reported as catalysts for the Wittig reaction starting from alcohols through a temporarily oxidized alcohol.<sup>28,29</sup> On the other hand, metal nanoparticles are not very common among the catalysts used for the one-pot olefination starting from alcohols; in fact, only NiNPs have been reported so far and the reaction was claimed to proceed without a standard redox step.<sup>30,31</sup> In this paper, beyond preparing efficient Wittig catalysts by very mild routes, it is worth noting that our evidence shows that the free aldehyde does not mediate the reaction, as these catalysts are unable to oxidize alcohols to the corresponding aldehydes. Perhaps, association of the alcohol at the ruthenium site occurs, just as it does in the Ley-Griffith<sup>32</sup> oxidation, but the reaction is aborted if the Wittig reagent is not present. The nature of the support as well as the highly dispersed anchored RuNP may play a crucial role since embedded RuNP in aluminum oxyhydroxide have been reported as catalysts for the same reaction producing  $\alpha,\beta$ -unsaturated esters mediated by the aldehyde.<sup>14</sup> The chemistry described here bears some resemblance to 'borrowing hydrogen' type mechanisms,<sup>28,31,33,34</sup> however, in this case, the aldehyde (the product of borrowing hydrogen from an alcohol) is never isolated or "free". Further, the borrowed hydrogen is not returned to the nascent double bond, but presumably to oxygen (that is essential) to form water. The tentative mechanism is depicted in Scheme 2 and shows the necessary alcohol oxidation and the olefination as coupled processes involving an activated alcohol on the ruthenium surface.

From the data shown in Table 2, the reaction leads always to the *E*-methyl cinnamate as the preferred isomer. Higher conversions were obtained when non-polar solvents such as toluene and CCl<sub>4</sub> were used. A very low yield was obtained when DMF (Table 2, entry 5) was used. While using THF, no conversion was achieved even under reflux for 18 h (Table 2, entry 6). Increasing the temperature from 80 to 110 °C did not result in an increase in the conversion (Table 2, entries 4 and 7). When the reaction was performed under air, the byproduct benzyl cinnamate was obtained together with a similar yield of the desired methyl cinnamate (Table 2, entry 9), whereas under N<sub>2</sub>, almost no reaction took place, even after increasing the temperature (Table 2, entry 8). When the percentage of Ru was increased up to 1.2%, the conversion increased up to 70% after 24 h; nevertheless, quantitative conversion could be obtained after 48 h (Table 2, entries 10 and 11). Blank experiments showed that the reaction does not occur without SRuNP (Table 2, entry 1) or when only the support was tested as a possible catalyst (Table 2, entry 2).

Table 3 shows that the steric hindrance plays an important role in the yield and selectivity of the reaction. The OMe substituent was evaluated in the *ortho*, *meta* and *para* positions of benzyl alcohol. When the OMe substituent was in *para* position, the donating effect of the substituent achieved quantitative conversion and excellent selectivity as shown by the *E/Z* ratio. However, the yield and selectivity decreased as steric hindrance increased (Table 3, entries 2 and 3). Even more, the very sterically hindered anthracene-9-methanol gave the desired product in only 40% yield the *E/Z* ratio being as low as 2:1 (Table 3, entry 5). The effect of an electron-withdrawing group in the *para* position decreases the yield and the *E/Z* ratio (Table 3, entry 4). In addition, in Table 3, entry 6, the ester was obtained, but eventually the alkene was hydrogenated to afford the saturated product, in accordance with previous results using [Ir(COD)Cl]<sub>2</sub>.<sup>33</sup> Table 4 showed that MCM-41 and SBA-15 type silica showed the same conversion. Nevertheless, Ru@MCM material was more selective toward the *E*-methylcinnamate isomer. This may reflect the smaller pore size of the MCM type silica, *i.e.*, 3 nm, against the 9 nm for SBA-15 type silica. Moreover, HMS solids showed lower conversions presumably due to their reduced accessible volume; it is common for metal to reduce the available volume, but the effect of ruthenium seems to be

**Scheme 2** Proposed mechanism for the alcohol oxidation-Wittig olefination showing alcohol oxidation and olefination as coupled processes.

quite large compared with Fe or Co.<sup>35</sup> With regard to the recyclability, all the catalysts conserved 50%–60% of their original activity upon second use.

## Conclusion

Three new materials based on MCM-41, SBA-15 and HMS type silica containing RuNP covalently attached to the structure have been prepared under very mild conditions; stirring a Ru(III) salt at room temperature in the presence of the solid grafted with APTES led to the formation of RuNP of 3 nm average size highly dispersed into the channels of the mesoporous silicas. The materials exhibited high catalytic activity in the alcohol oxidation–Wittig olefination of different benzyl alcohols. Interestingly, the reaction does not appear to involve the intermediacy of the aldehyde, the usual Wittig reagent.

## Acknowledgements

Thanks are due to the Natural Sciences and Engineering Council of Canada and the Canadian Foundation for Innovation for their generous support. M.L. Marin thanks the Universitat Politècnica de Valencia (Programa de Apoyo a la Investigación y Desarrollo) for its financial support. Thanks are due to Dr. Yun Liu for advice on XPS interpretation.

## Notes and references

- G. C. F. Cavani, S. Perathoner and F. Trifiro, *Sustainable Industrial Chemistry*, Wiley-VHC, Weinheim, 2009.
- V. Hulea, D. Brunel, A. Galarneau, K. Philippot, B. Chaudret, P. J. Kooyman and F. Fajula, *Microporous Mesoporous Mater.*, 2005, **79**, 185.
- A. Taguchi and F. Schüth, *Microporous Mesoporous Mater.*, 2005, **77**, 1.
- D. Trong On, D. Desplantier-Giscard, C. Danumah and S. Kaliaguine, *Appl. Catal., A*, 2001, **222**, 299; Y. Wu, L. Zhang, G. Li, C. Liang, X. Huang, Y. Zhang, G. Song, J. Jia and C. Zhixiang, *Mater. Res. Bull.*, 2001, **36**, 253.
- J. Garcia-Martinez, N. Linares, S. Sinibaldi, E. Coronado and A. Ribera, *Microporous Mesoporous Mater.*, 2009, **117**, 170.
- A. I. Carrillo, J. García-Martínez, R. Llusar, E. Serrano, I. Sorribes, C. Vicent and J. Alejandro Vidal-Moya, *Microporous Mesoporous Mater.*, 2012, **151**, 380.
- E. Iglesia, S. L. Soled, R. A. Fiato and G. H. Via, *J. Catal.*, 1993, **143**, 345.
- D. P. VanderWiel, M. Pruski and T. S. King, *J. Catal.*, 1999, **188**, 186.
- V. Mazzieri, F. Coloma-Pascual, A. Arcoya, P. C. L'Argentière and N. S. Figoli, *Appl. Surf. Sci.*, 2003, **210**, 222.
- J. Zhang, H. Xu, Q. Ge and W. Li, *Catal. Commun.*, 2006, **7**, 148.
- F. Su, L. Lv, F. Y. Lee, T. Liu, A. I. Cooper and X. S. Zhao, *J. Am. Chem. Soc.*, 2007, **129**, 14213.
- P. A. Byrne and D. G. Gilheany, *Chem. Soc. Rev.*, 2013, **42**, 6670.
- C. J. O'Brien, J. L. Tellez, Z. S. Nixon, L. J. Kang, A. L. Carter, S. R. Kunkel, K. C. Przeworski and G. A. Chass, *Angew. Chem., Int. Ed.*, 2009, **48**, 6836.
- E. Y. Lee, Y. Kim, J. S. Lee and J. Park, *Eur. J. Org. Chem.*, 2009, 2943.
- Z. Luan, M. Hartmann, D. Zhao, W. Zhou and L. Kevan, *Chem. Mater.*, 1999, **11**, 1621.
- W. Zhang, T. R. Pauly and T. J. Pinnavaia, *Chem. Mater.*, 1997, **9**, 2491.
- A. I. Carrillo, E. Serrano, R. Luque and J. G. Matinez, *Chem. Commun.*, 2010, **46**, 5163.
- K. R. Chary and C. Srikanth, *Catal. Lett.*, 2008, **128**, 164.
- J. Chen, J. Zhou, R. Wang and J. Zhang, *Ind. Eng. Chem. Res.*, 2009, **48**, 3802.
- A. I. Carrillo, N. Linares, E. Serrano and J. García-Martínez, *Mater. Chem. Phys.*, 2011, **129**, 261.
- I. Kusunoki and Y. Igari, *Appl. Surf. Sci.*, 1992, **59**, 95; H. Zarrin, D. Higgins, Y. Jun, Z. Chen and M. Fowler, *J. Phys. Chem. C*, 2011, **115**, 20774.
- W. Tu and H. Liu, *J. Mater. Chem.*, 2000, **10**, 2207.
- X. Yan, H. Liu and K. Y. Liew, *J. Mater. Chem.*, 2001, **11**, 3387.
- J. D. S. Newman and G. J. Blanchard, *Langmuir*, 2006, **22**, 5882.
- D. T. Marquez, A. I. Carrillo and J. C. Scaiano, *Langmuir*, 2013, **29**, 10521.
- W.-H. Kim, I. S. Park and J. Park, *Org. Lett.*, 2006, **8**, 2543.
- R. Robiette, J. Richardson, V. K. Aggarwal and J. N. Harvey, *J. Am. Chem. Soc.*, 2006, **128**, 2394.
- M. G. Edwards, R. F. R. Jazzar, B. M. Paine, D. J. Shermer, M. K. Whittlesey, J. M. J. Williams and D. D. Edney, *Chem. Commun.*, 2004, 90.
- S. Burling, B. M. Paine, D. Nama, V. S. Brown, M. F. Mahon, T. J. Prior, P. S. Pregosin, M. K. Whittlesey and J. M. J. Williams, *J. Am. Chem. Soc.*, 2007, **129**, 1987.
- F. Alonso, P. Riente and M. Yus, *Eur. J. Org. Chem.*, 2009, 6034.
- F. Alonso, P. Riente and M. Yus, *Acc. Chem. Res.*, 2011, **44**, 379.
- W. P. Griffith, S. V. Ley, G. P. Whitcombe and A. D. White, *J. Chem. Soc., Chem. Commun.*, 1987, 1625.
- P. J. Black, M. G. Edwards and J. M. J. Williams, *Eur. J. Org. Chem.*, 2006, 4367.
- T. D. Nixon, M. K. Whittlesey and J. M. J. Williams, *Dalton Trans.*, 2009, 753.
- L. F. F. P. G. Bragança, M. Ojeda, J. L. G. Fierro and M. I. P. da Silva, *Appl. Catal., A*, 2012, **423–424**, 146.